# Gamma Rays from Ultra-High Energy Cosmic Rays in Cygnus A

Armen Atoyan[1] and Charles D. Dermer[2]


## ABSTRACT

Ultra-high energy cosmic rays (UHECRs) accelerated in the jets of active galactic nuclei can accumulate in high magnetic field, $\sim 100$ kpc-scale regions surrounding powerful radio galaxies. Photohadronic processes involving UHECRs and photons of the extragalactic background light make ultra-relativistic electrons and positrons that initiate electromagnetic cascades, leading to the production of a $\gamma$-ray synchrotron halo. We calculate the halo emission in the case of Cygnus A and show that it should be detectable with the Fermi Gamma ray Space Telescope and possibly detectable with ground-based $\gamma$-ray telescopes if radio galaxies are the sources of UHECRs.


*Subject headings:* Galaxies: individual (Cygnus A) — cosmic rays: theory — galaxies: active — galaxies: jets — radiation processes: nonthermal

## 1. Introduction

Active galactic nuclei (AGN) and gamma-ray bursts are considered as two of the most plausible classes of astrophysical accelerators of extragalactic ultra-high energy cosmic rays (UHECRs; see, e.g., Halzen & Hooper 2002). The recent report of the Pierre Auger Collaboration (2007) about clustering of the arrival directions of UHECRs with energies $E \gtrsim 6 \times 10^{19}$ eV within $\approx 3^\circ$ of the directions to AGN at distances $d \lesssim 75\,$Mpc strongly suggests that effective production of cosmic rays with energies $E \sim 10^{20}\,$eV takes place in at least one of these source classes. Because of photohadronic GZK interactions of protons or ions with the CMB radiation, the study of super-GZK UHECRs from sources at $d \gtrsim 100\,$Mpc becomes impossible with cosmic-ray detectors like the Pierre Auger Observatory (Harari et al. 2006). Powerful AGN, as well as GRBs, are mostly located at larger distances.

Relativistic beams of energy from the central nuclei of AGN are thought to power the multi-kpc scale radio lobes of powerful galaxies and form an extended cavity (Scheuer 1974). Acceleration of UHECRs in the compact inner jets of the radio galaxy on the sub-parsec scale, followed by production of collimated beams of ultra-high energy neutrons and gamma-rays, provides a specific

[1]Department of Mathematics, Concordia University, 1455 de Maisonneuve Blvd. West, Montreal, Quebec H3G 1M8, Canada; atoyan@mathstat.concordia.ca

[2]Space Science Division, Code 7653, Naval Research Laboratory, Washington, DC 20375-5352, USA; charles.dermer@nrl.navy.mil

mechanism to transport energy to the radio lobes and cavity (Atoyan & Dermer 2003). When the neutron-decay UHECR protons interact with the extragalactic background light (EBL), which is dominated by the CMB radiation, ultra-relativistic electrons (including positrons) and $\gamma$ rays with $E \gtrsim 10^{18}\,\mathrm{eV}$ are produced. Such secondaries can initiate pair-photon cascades to form large multi-Mpc scale halos of GeV/TeV radiation due to Compton and synchrotron processes (Aharonian et al. 1994; Aharonian 2002; Inoue et al. 2005).

In this Letter, we predict that synchrotron GeV fluxes from UHECR AGN sources are detectable with the Fermi Gamma ray Space Telescope (FGST; formerly the Gamma ray Large Area Space Telescope, GLAST) if UHECRs are captured in the vicinity of radio galaxies for sufficiently long times. Magnetic fields at the $\gtrsim \mu$G level in the kpc – Mpc vicinity from the AGN core are required to isotropize UHECRs accelerated by jets of radio galaxies. Indeed, for protons with energy $E \equiv 10^{20} E_{20}\,\mathrm{eV}$, the mean magnetic field $B$ required to provide gyroradii smaller than size $r$ is $B \gtrsim 10^{-4} E_{20} r_{\rm kpc}^{-1}\,\mathrm{G}$, where $r_{\rm kpc} = r/1\,\mathrm{kpc}$ is the spatial scale where the isotropization occurs.

Here we consider the specific case of the powerful radio galaxy Cygnus A, where the mean magnetic field in the surrounding cavity could reach 10 – 100 $\mu$G at 100 kpc scales. Its properties are considered in Section 2, and calculations are presented in Section 3. We summarize in Section 4.

## 2. Model Parameters

Magnetic fields $B \gtrsim 1\,\mu G$ could be present at $\lesssim 1\,\mathrm{Mpc}$ scales in clusters of galaxies (Kim et al. 1990; Feretti et al. 1995; Ferrari et al. 2008). Even higher magnetic fields, $B \sim 10^{-4}\,\mathrm{G}$, could be present in the $r \lesssim 100\,\mathrm{kpc}$ vicinity of cD galaxies near the center of galaxy clusters like the powerful radio galaxy Cyg A (Wilson et al. 2006). In such magnetic fields, synchrotron radiation of electrons with $E \sim 10^{18}\,\mathrm{eV}$ produced in photomeson interactions is in the TeV domain. Furthermore, synchrotron radiation of lower energy electrons produced in $p + \gamma \to p + e^+ + e^-$ interactions by UHECRs extends to the GeV domain and could become detectable with the Fermi Telescope. Here we consider the detectability of these fluxes from the powerful and well-studied radio galaxy Cyg A.

### 2.1. Power of the Cosmic Ray Accelerator

Observations of Cygnus A ($z = 0.056$, luminosity distance $\simeq 240\,\mathrm{Mpc}$) by the Chandra X-ray Observatory show that the central $\sim 60$ kpc $\times$ 120 kpc size luminous prolate spheroidal region of Cygnus A, called a "cavity," can be understood as a shock expanding into the accretion cooling-flow gas (Wilson et al. 2006). The kinetic power of expansion of this X-ray cavity deduced by Wilson et al. (2006) is $L_{\rm exp} \approx 1.2 \times 10^{46}\,\mathrm{erg\,s^{-1}}$. This is much larger than the total radio luminosity $L_{\rm lobes} \approx 10^{45}\,\mathrm{erg\,s^{-1}}$ of the two bright radio lobes of Cygnus A (Perley et al. 1984). The value of

$L_{\rm exp}$ should be considered as a *lower* limit to the overall power $L_{CR}$ of cosmic rays injected into the cavity, if the cosmic-ray power is assumed to drive the expansion of the cavity. A few times larger power, $L_{\rm CR} \sim 4 \times 10^{46}$ ergs s$^{-1}$ therefore seems a reasonable assumption.

This value is in a good agreement with the "neutral beam" model (Atoyan & Dermer 2001, 2003), which explains the collimated relativistic X-ray jets that remain straight up to $\simeq 1$ Mpc distances in sources such as Pictor A (Wilson, Young, and Shopbell 2001) as the result of energy transport by beams of UHE neutrons and gamma-rays. These linear X-ray features, surrounded by a broader and less collimated radio structure in Pictor A, and coincident with narrow radio structures exhibiting bends and deflections in Cyg A (Carilli et al. 1996; Steenbrugge & Blundell 2008), terminate in X-ray hot spots. Because of the large inclination angle, the X-ray jets in Cyg A cannot be detected. However detection of bright X-ray hot spots located at $\simeq 60\,$kpc distances on opposite sides of the nucleus (Wilson et al. 2006) strongly implies production of collimated X-ray jets also in Cyg A.

Detailed calculations in the framework of this model show that neutral beams of ultrarelativistic neutrons and $\gamma$ rays, produced by the compact relativistic jets in the central sub-parsec scale environment of FRII galaxies, can take a few percent of the total power of this inner jet. That energy is then deposited, after $\beta$-decay of neutrons $n \to p + e + \nu_e$, on distance scales $l_d \simeq E_{20}\,$Mpc, and also via photopair production of UHE gamma-rays through the process $\gamma + \gamma \to e^- + e^+$. These secondary charged relativistic particles initially form a beam in the same direction as the jet, and can effectively interact with and transfer momentum and energy to the ambient magnetized medium, and thus can be the basic energy reservoir for the jet at large distances from Cyg A. The total radio luminosity $\simeq 9 \times 10^{44}\,{\rm erg\,s^{-1}}$ detected from the lobes of Cyg A (Carilli & Barthel 1996; Wilson et al. 2006) imposes the minimum power requirement for the beam. Given the $\sim (2-3)\%$ efficiency of neutral beam production, the acceleration power of the CRs in the relativistic inner jet must be $L_{\rm CR} \gtrsim (3-5) \times 10^{46}\,{\rm erg/s}$. This power is then released in CRs when the inner jet decelerates to subrelativistic speeds in the dense medium at kpc scales. This scenario is in agreement with the assumption that the expansion of the cavity against the cooling flow observed (Smith et al. 2002) at distances $\lesssim 70$ – 100 kpc is powered by cosmic-ray pressure.

Protons are accelerated in the inner jet of Cyg A to a maximum energy $E_{max} \approx 10^{20}$ eV, consistent with size scales and magnetic fields inferred from a synchrotron model of blazars corresponding to Cyg A if observed along its jet. This value of $E_{max}$ is in accord with the spatial extent of the X-ray hot spot where the large-scale jet terminates due to the $\beta$-decay of the remaining high-energy neutrons in the beam. At this distance, the injection power from the decaying neutrons is balanced by the ram pressure of the external medium. Thus, for $l_d \sim 100$ kpc-long jets originating from neutral beams, the inner jets must accelerate protons to $E \gtrsim 10^{19}$eV. In our model, we assume that acceleration of UHECRs to $E \sim 10^{20}$ eV occurs.

### 2.2. Magnetic Field Strength

The lower limit to the equipartition magnetic field in the radio lobes of Cyg A inferred from radio observations is $\approx 60\,\mu$G (Carilli et al. 1991). The equipartition magnetic field in the cavity derived from X-ray observations is $B \simeq 120\,\mu$G (Wilson et al. 2006). Moreover, the field outside the cavity could also be very high given the large thermal electron energy density inferred from the X-ray emission at $\lesssim 8'$ or in the $\lesssim 500\,$kpc environment around Cyg A. The pressure of hot thermal gas decreases from $2.3 \times 10^{-10}$ erg cm$^{-3}$ in the regions near the cavity to $\lesssim 10^{-11}$ erg cm$^{-3}$ at distances $\gtrsim 500$ kpc from the center of Cyg A (Smith et al. 2002). The corresponding equipartition magnetic fields would then vary from $\sim 80\,\mu$G to $\sim 15\,\mu$G at the periphery of this region.

### 2.3. Injection Age

The duration of injection of UHECRs, i.e., the jet injection age, represents one of the important parameters of the model. Wilson et al. (2006) find that the expansion age of the cavity, determined from the speed of the shock deduced from the analysis of X-ray data, is $t \sim 3\times10^7$ yr. The injection age can be larger than this dynamical age because the derived value neglects the magnetic-field pressure of the intracluster medium (ICM) upstream of the shock, as recognized by Wilson et al. (2006). Also, this age estimate neglects the infall velocity of the cooling flow. For the total mass $M \approx 2 \times 10^{13} M_\odot$ enclosed at $r \leq 50\,$kpc distances (Smith et al. 2002), the virial speed $v_{\rm vir} \approx c/\sqrt{r/r_{\rm S}} \cong 2000\,$km/s, where $r_{\rm S} = 2GM/c^2 \approx 6 \times 10^{18}\,$cm is, formally, the Schwarzschild radius for the total mass $M$. The value of $v_{\rm vir}$ gives a measure of the accretion/cooling flow velocities at radius $r$, and is comparable to the average $\sim 1500\,$km/s speed of the shock derived by Wilson et al. (2006) in the rest frame of the fluid upstream of the shock. These factors can significantly decrease the speed of expansion of the cavity in the stationary frame, so that the real injection age of the cavity can be significantly larger than the age inferred by Wilson et al. (2006).

We now estimate the age of activity of the black-hole jet from energetics arguments. The inferred jet power, $L_{jet} \simeq 4 \times 10^{46}\,$erg/s, corresponds to $\simeq 12\%$ of the Eddington luminosity for a black-hole mass $M_{\rm BH} \simeq 2.5\times10^9 M_\odot$ in Cygnus A (Tadhunter et al. 2003). To produce such power, the black hole should accrete mass at the rate $\dot{M} = L_{jet}/\eta c^2 = (7/\eta_{-1}) M_\odot\,{\rm yr}^{-1}$ with an efficiency $\eta = 10^{-1}\eta_{-1}$, with $\eta_{-1} \approx 1$. The age of the central black hole is estimated by its growth time $t \simeq M_{\rm BH}/\dot{M} = 3.6\times10^8\eta_{-1}\,$yr, giving an upper estimate for the jet's age as the jet might be active for only a fraction of the BH growth phase. These estimates are in accord with the characteristic jet age $t \sim 10^8$ yr inferred from a model for "cocoon" (or cavity) dynamics by Begelman & Cioffi (1989).

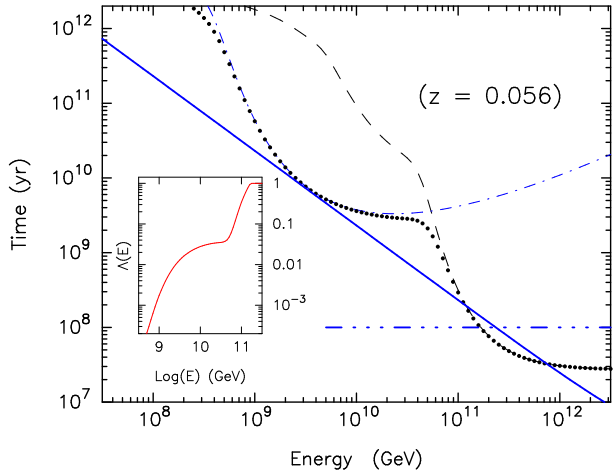


Fig. 1.— Comparison of timescales for energy losses through photomeson (dashed curve) and photopair (dot-dashed curve) production, confinement (solid line) with $B = 20$ $\mu$G and $r = 500$ kpc, and injection with $t_{age} = 10^8$ yrs (triple-dot-dashed line). The inset shows the fraction $\Lambda(E)$ of energy extracted by photohadronic processes from UHECRs with energy $E$.

### 2.4. Cosmic Ray Diffusive Confinement Time

The maximum confinement timescale $t_{conf}$ of UHECRs in a source of size $r$ is given in the Bohm diffusion approximation by $t_{conf} \cong r^2/2D_{\rm B}$, where the Bohm diffusion coefficient $D_{\rm B} = cr_{\rm L}/3$, and $r_L \cong E/QB$ is the Larmor radius of a particle with charge $Q$. From this expression we obtain the UHECR proton confinement time

$$t_{conf} \cong 0.95 \times 10^7 \ (r/100 \ {\rm kpc})^2 E_{20}^{-1} \ (B/20 \ \mu{\rm G}) \ {\rm yr} \ . \tag{1}$$

For $r \sim 50$ kpc and $B \cong 120$ $\mu$G, $t_{conf} \cong 15$ Myr for $\approx 10^{20}$ eV protons.

Fig. 1 compares timescales $t_{loss}$ for energy losses due to photomeson and photopair production with values of $t_{conf}$ for characteristic parameters $r = 500$ kpc and $B = 20$ $\mu$G in the region surrounding Cyg A. Also shown is the value of $t_{age} = 10^8$ yrs for the assumed injection age. The fraction of energy of accelerated protons that could be extracted is given by $\Lambda(E) = \min(t_{conf}, t_{loss}, t_{age})/t_{loss}$. This figure shows that $\gtrsim 3\%$ of the total energy of UHECRs with $E \gtrsim 3 \times 10^{18}$ eV can be extracted through photohadronic processes. Because of the increased confinement time and the much lower production threshold for photopair than photomeson processes, the photopair process can make a comparable or dominant contribution to the electromagnetic channel compared to photomeson processes.

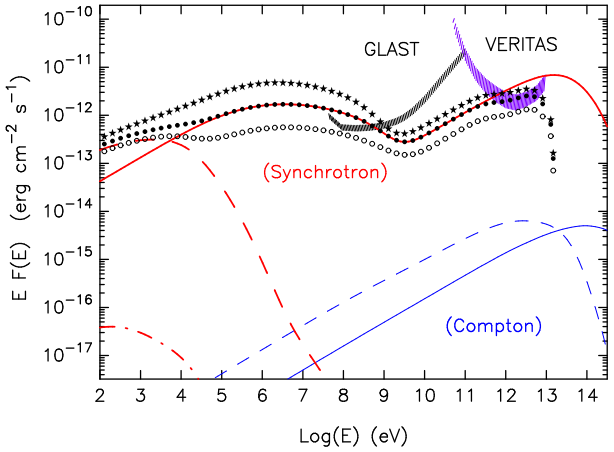


Fig. 2.— Fluxes from the electromagnetic cascade initiated within 0.5 Mpc distances from the core of Cyg A, assuming an average magnetic field $B = 20$ $\mu$G in the cavity. The total injection power of UHECR protons is $4 \times 10^{46}$ erg/s. The photon fluxes expected for $t_{age} = 30$ Myr, 100 Myr and 300 Myr are shown by the open dots, full dots and stars, respectively. The solid, dashed, and dot-dashed curves show three generations of synchrotron (heavy curves) and Compton (light curves) cascade radiations in the case of $t = 100$ Myr. Note that the third generation of Compton cascade radiation is too weak to appear on the plot. Sensitivities for the FGST and VERITAS are also shown.

## 3. Results

Fig. 2 shows $\gamma$-ray fluxes calculated for the electromagnetic cascade initiated by the injection of $4 \times 10^{46}$ erg s$^{-1}$ of UHECR protons into the cavity, and further cosmic ray interactions with the EBL in the $r = 0.5$ Mpc region surrounding Cyg A. Even though the EBL is dominated by the CMBR, interactions with the diffuse infrared/optical radiation are also included in the calculations, using the EBL of Primack et al. (2005). The injection spectrum of UHECR protons is a power-law with an $\alpha = -2.1$ number spectral index with a low-energy cutoff at $E = 1$ TeV and a high-energy exponential cutoff at $E = 3 \times 10^{20}$ eV. We assume a mean magnetic field $B = 20$ $\mu G$. Escape of particles is given by the Bohm diffusion approximation in a single zone model. The method of calculation follows the approach described by Atoyan & Dermer (2003).

The solid, dashed, and dot-dashed curves in Fig. 2 show the contributions to the fluxes from the photohadronic secondary electrons and the first two generations of cascade electrons for injection ages $t_{age} = 10^8$ yr. The secondary electrons also include the electrons from $\pi^0$-decay $\gamma$ rays that convert promptly into electron-positron pairs inside the source. In the strong magnetic field of the Cyg A environment, the Compton flux is dominated by synchrotron radiation from the photohadronic secondaries and the first generation of cascade electrons.

The open dots, full dots and stars in Fig. 2 show the received $E \cdot F(E)$ spectral energy fluxes for

injection ages $t_{age} = 30\,\mathrm{Myr}$, 100 Myr and 300 Myr, respectively. The lower and higher energy peaks in the spectral energy distributions primarily result from photopair and photomeson processes, respectively. The sensitivities for a one-year, $5\sigma$ detection of a point source with the FGST in the scanning mode,[1] and for a 50 hour, $5\sigma$ detection with VERITAS are shown. The lower bound of the VERITAS sensitivity applies to a point source, and the upper bound to a source of $25'$ extent.

## 4. Discussion and Conclusions

If the radio lobes of Cyg A are powered by UHECR production from the inner pc-scale jets, then trapping of these particles in the surrounding strong magnetic-field region leads to the production of secondary $\gamma$ rays that should be significantly detected with the FGST in one year of observation if the jet injection age is $\gtrsim 100$ Myr. If radio galaxies are not the sources of UHECRs, then Cygnus A will not be detected by the FGST. Cyg A could also be detected with VERITAS in a 50 hour pointing, depending on the duration of activity of the central engine and the level of the EBL.

Detection of GeV $\gamma$ rays from Cyg A with the FGST might also be expected to arise from other processes. The $\sim$ 10 – 100 GeV radio-emitting electrons from the lobes of radio galaxies will Compton-scatter CMB photons to MeV – GeV energies (e.g., Cheung 2007). For the strong magnetic field, $\approx 60\ \mu$G, in the lobes of Cyg A, however, the ratio of the magnetic-field to CMBR energy densities is $\approx 400$. Thus the total energy flux of Compton-scattered CMBR from Cyg A is $\approx 10^{45}$ erg s$^{-1}$/$[400(4\pi d^2)] \cong 4 \times 10^{-13}$ ergs cm$^{-2}$ s$^{-1}$, with the $E \cdot F(E)$ flux a factor of $\sim 5$ – 10 lower. As can be seen from Fig. 2, this process is almost two orders of magnitude below the UHECR-induced synchrotron flux, and well below the FGST sensitivity.

Inoue et al. (2005) considered fluxes expected from the $\lesssim 1\,\mathrm{Mpc}$ halos of clusters of galaxies with weaker magnetic fields, $B \simeq 0.1\text{-}1\,\mu$ G in a model where acceleration of UHECRs occurs in accretion shocks in the cluster. Because of lower maximum energies of accelerated protons, $E \lesssim 10^{19}\,\mathrm{eV}$, and lower magnetic fields, this model predicts hard spectral fluxes of Compton origin peaking at TeV energies. Gabici & Aharonian (2005) predicted that synchrotron radiation from $\gtrsim 10^{18}\,\mathrm{eV}$ electrons is produced by secondaries of UHECRs that leave the acceleration region and travel nearly rectilinearly through weak intergalactic magnetic fields at the level $B \sim 10^{-7} - 10^{-9}\,\mathrm{G}$. These sources would appear as point-like quiescent GeV – TeV sources with spectra in the GeV domain as hard as $\alpha \cong -1.5$, and very soft, $\alpha \lesssim -3$ spectra in the 100 GeV – TeV domain.

In contrast to both these models, we predict soft 0.1 – 1 GeV spectra with $\alpha \cong -2.5$ and hard, $\alpha \cong -2$ spectra at TeV energies due to the much higher magnetic field in the confinement region. These models can be clearly distinguished if Cygnus A is resolved by the Fermi Gamma ray Space Telescope or the ground-based $\gamma$-ray telescopes, as the emission region in our model subtends an

[1] www-glast.slac.stanford.edu/software/IS/glast_lat_performance.htm; note that the FGST sensitivity will be somewhat poorer than shown at the 5.76° galactic latitude of Cyg A due to Galactic background.

angle $\approx 10'$.

Because Cygnus A lies outside the GZK horizon, only UHECRs with energy below the GZK energy could be correlated with this source. Other closer FRII radio galaxies that are correlated with the arrival directions of UHECRs are, however, candidate sources of $\gamma$ rays made through the mechanism proposed here. IGR J21247+5058 at $z = 0.02$ or $d \approx 80$ Mpc, recently discovered with INTEGRAL (Molina et al. 2007), is 2.1 degrees away from a HiRes Stereo event with $E > 56$ EeV (C. C. Cheung, private communication, 2008).[2] PKS 2158-380 at $\approx 140$ Mpc is also within 3.2° degrees of an Auger UHECR with $E > 57$ EeV (Moskalenko et al. 2008). By comparison with Cyg A, these are low luminosity FRIIs, and their predicted flux level will require detailed modeling for each source, as done here for Cyg A. Variability of $\gamma$-ray emission would rule out our model.

We thank Vladimir Vassiliev for discussion and providing the VERITAS sensitivities, Teddy Cheung and Felix Aharonian for important comments, and the referee for a detailed report. The work of AA and visits to NRL were supported by the GLAST Interdisciplinary Science Investigation Grant DPR-S-1563-Y. The work of CDD is supported by the Office of Naval Research.

## REFERENCES

Abbasi, R. U., et al. 2008, ArXiv e-prints, 804, arXiv:0804.0382

Aharonian, F. A., Coppi, P. S., Völk, H. J. 1994, ApJ, 423, L5

Aharonian, F. A. 2002, MNRAS, 332, 202

Atoyan, A. M., & Aharonian, F. A. 1999, MNRAS, 302, 253

Atoyan, A., and Dermer, C. 2001, PRL 87, 221102

Atoyan, A., and Dermer, C. 2003, ApJ, 586, 79

Begelman, M. C., & Cioffi, D. F. 1989, ApJ, 345, L21

Carilli, C., Perley, R., Bartel, N., & Dreher, J. 1996, in Cygnus A – Study of a Radio Galaxy, eds. by C.L. Carilli and D.E. Harris (Cambridge: Cambridge University Press), 76

Carilli, C. L., Perley, R. A., Dreher, J. W., & Leahy, J. P. 1991, ApJ, 383, 554

Carilli, C. L., & Barthel, P. D. 1996, A&A Rev., 7, 1

[2]This radio galaxy was identified as such only recently and would not have appeared in the list of AGN used by the HiRes collaboration in their correlation study (Abbasi et al. 2008).

Cheung, C. C. 2007, The First GLAST Symposium, S. Ritz, P. Michelson, & C. Meegan, eds. (AIP: New York) 921, 325

Dermer, C. D., & Atoyan, A. 2004, ApJ, 611, L9

Feretti, L., Dallacasa, D., Giovannini, G., & Tagliani, A. 1995, A&A, 302, 680

Ferrari, C., Govoni, F., Schindler, S., Bykov, A. M., & Rephaeli, Y. 2008, Space Science Reviews, 134, 93

Gabici, S., & Aharonian, F. A., 2005, Phys. Rev. Lett. 95, 251102

Halzen, F., & Hooper, D. 2002, Reports of Progress in Physics, 65, 1025

Harari, D., Mollerach, S., & Roulet, E. 2006, J. Cosmology and Astroparticle Physics, 11, 12

Inoue, S., Aharonian, F. A., and Sugiyama, N. 2005, ApJ, 628, L9

Kim, K.-T., Kronberg, P. P., Dewdney, P. E., & Landecker, T. L. 1990, ApJ, 355, 29

Molina, M., et al. 2007, MNRAS, 382, 937

Moskalenko, I. V., Stawarz, L., Porter, T. A., & Cheung, C. C. 2008, ArXiv e-prints, 805, arXiv:0805.1260

Mücke, Rachen, J.P., A., Engel, R., Protheroe, R.J., and Stanev, T. 1999, Pub. Astron. Soc. Australia, 16, 160

Perley, R. A., Dreher, J. W., & Cowan, J. J. 1984, ApJ, 285, L35

The Pierre Auger Collaboration, et al., 2007, Science, 318, 938

Primack, J. R., Bullock, J. S., & Somerville, R. S. 2005, High Energy Gamma-Ray Astronomy, 745, 23

Scheuer, P. A. G. 1974, MNRAS, 166, 513

Smith, D. A., Wilson, A. S., Arnaud, K. A., Terashima, Y., & Young, A. J. 2002, ApJ, 565, 195

Steenbrugge, K. C., & Blundell, K. M. 2008, MNRAS, 388, 1457

Tadhunter, C., Marconi, A., Axon, D., Wills, K., Robinson, T. G., & Jackson, N. 2003, MNRAS, 342, 861

Wehrle, A. E. et al. 1998, ApJ, 497, 178

Wilson, A. S., Young, A. J., and Shopbell, P. L. 2001, ApJ, 547, 740

Wilson, A., et al. 2006, ApJ, 644, L9